# Reactions of Biological Oxidants with Selenourea: Formation of Redox Active Nanoselenium

**B. Mishra,[†] P. A. Hassan,[‡] K. I. Priyadarsini,*[,†] and Hari Mohan[†]**

*Radiation Chemistry and Chemical Dynamics Division and Novel Materials and Structural Chemistry Division, Bhabha Atomic Research Centre, Trombay, Mumbai 400085, India*

*Received: March 14, 2005; In Final Form: May 6, 2005*

Reactions of biological oxidizing agents, such as hydroxyl radicals ($^{\bullet}OH$), singlet oxygen ($^1O_2$), hydrogen peroxide ($H_2O_2$), and peroxynitrite ($ONOO^-$) with selenourea were studied. The kinetics of the reactions was followed using time-resolved techniques, and the bimolecular rate constants were determined. In all these reactions, under aerated conditions, elemental red selenium was produced as one of the reaction products. The average size of the selenium particles could be controlled and stabilized in the range of 20−100 nm with the addition of bovine serum albumin (BSA) or sodium dodecyl sulfate (SDS). The particles were characterized by dynamic light scattering studies (DLS), which revealed that the size and distribution of the particles depended mainly on the amount of selenourea undergoing oxidation. Other factors such as the nature of the oxidant and the concentration of the stabilizer also are important in stabilizing the particles. Nanoselenium-reduced $ABTS^{\bullet-}$ to colorless $ABTS^{2-}$ (ABTS = 2,2′-azinobis(3-ethylbenzothiazoline-6-sulfonate) and oxidized dichlorodihydrofluoresecein diacetate (DCFA) to fluorescent dichlorofluorescein (DCF) indicating its ability to participate in redox and free radical reactions. The reactivity of selenium nanoparticles with these systems varied linearly with the surface area of the particles. The studies demonstrate that selenourea undergoes oxidation with both one-electron and two-electron oxidants to produce elemental selenium, which, on stabilization to nanometer size, exhibits size-dependent redox activity.

## Introduction

Selenium is an essential trace element for animals and humans, being a constituent of redox active enzymes such as glutathione peroxidase and glycine reductase, etc.[1−3] Selenium compounds also exhibit antioxidant and radioprotecting activity and are free radical scavengers.[4−6] Selenium compounds employed for such studies have mostly selenium in the oxidation states of +6, +4, and −2; on the other hand there are only a few reports on elemental selenium with zero oxidation number ($Se^0$). One of the reasons for these limited studies is due to the notion that colloidal selenium has very low bioavailability and biological activity.[1,7,8] Recently it has been reported that particles of selenium stabilized to nanometer size exhibit high biochemical activity and have improved bioavailability.[9−13] In biological systems, several bacteria are known to produce nanoselenium during the detoxification of selenium compounds.[7] A few studies on the bioactivity of nanoselenium have been reported in the literature. For example, protein conjugates of nanoselenium have been reported to be cytotoxic toward tumor cells.[9] Zhang et al. studied the toxicity of nanoselenium in cellular systems and showed that nanoselenium has lower toxicity than sodium selenite, and they also did not find any size effect on the induction of seleno enzymes.[10,11] Nanoselenium has also been studied for antioxidant activity and free radical reactions.[12,13] Some studies on the biological activities of nanoselenium have been listed by Shanghai Stone Nano Technology Port Ltd.[14]

In this paper, we present in situ generation of nanoselenium by the oxidation of selenourea by biological oxidants. Selenourea is one of the simplest of selenium compounds and has been shown to exhibit radioprotecting ability.[5,15] Selenourea has been tested in *Escherichia Coli* (*E. coli*) and was found to be nontoxic up to 0.1 M concentration without any irradiation and up to 0.05 M after irradiation with 150 krads.[5] It is also reported that colloidal selenium produced in such reactions is either biologically inactive or sometimes acts as a sensitizer.[15] Since oxidative processes (oxidative stress) are associated with most of the pathological conditions and also exposure to radiation,[16] oxidative transformation of selenourea into elemental selenium of nanometer size (nanoselenium) can be used alternatively for modulating oxidative stress to advantageous therapeutic purposes. With this objective, we studied the oxidation of selenourea by important biological oxidants such as $^{\bullet}OH$ radicals, hydrogen peroxide, peroxynitrite, and singlet oxygen to produce nanoselenium. Attempts have also been made to characterize them and study their redox reactions.

Earlier, using pulse radiolysis technique, we reported the reactions of hydroxyl radicals with selenourea,[17] where formation of radical cations and their subsequent dimerization has been identified. Further these solutions were converted to red colloidal solution due to the formation of elemental selenium particles ($Se_n^0$). The rate constant for the reaction of hydroxyl radicals was determined to be $(9.0 \pm 0.9) \times 10^9\ M^{-1}\ s^{-1}$.

Other specific one-electron oxidants such as $N_3^{\bullet}$ radicals showed similar reactions and produced the same intermediates and products.[17] From these studies it is evident that selenourea on oxidation under aerobic conditions produces elemental selenium. We investigated the reactions of other biological oxidants such as $H_2O_2$, peroxynitrite, and singlet oxygen with selenourea. $H_2O_2$ is produced in the cells by the dismutation of superoxide ion, while peroxynitrite is produced in vivo by the

* To whom correspondence should be addressed. Fax: 91-22-25505151. E-mail: kindira@apsara.barc.ernet.in.

[†] Radiation and Chemistry and Chemical Dynamics Division.

[‡] Novel Materials and Structural Chemistry Division.

10.1021/jp051328n CCC: $30.25 
Published on Web 06/15/2005

reaction of nitric oxide with superoxide ion and singlet oxygen is produced during peroxyl radical reactions and also during photodynamic action.[14−16] All these species have been found to be responsible for the induction of oxidative stress[16,18] and have been implicated in several diseases.

## Experimental Section

Selenourea, 2,2′-azinobis(3-ethylbenzothiazoline-6-sulfonic acid diammonium salt) ($ABTS^{2-}$), dichlorodihydrofluorescein diacetate (DCFA), bovine serum albumin (BSA), sodium dodecyl sulfate (SDS), and hematoporphyrin were obtained from the local markets and were of the highest purity available (>95%). $H_2O_2$ concentration was estimated by iodine method.[19] Peroxynitrite was prepared by the ozonolysis of alkaline sodium azide solutions according to the reported procedure.[20] The concentration of peroxynitrite was estimated by measuring the absorbance at 302 nm using the extinction coefficient value of 1670 $M^{-1}$ $cm^{-1}$. Kinetics of the reactions of $H_2O_2$ and peroxynitrite with selenourea was studied using stopped-flow kinetic spectrometer (model SX 18 MV from Applied Photophysics, U.K.) in single mixing mode. The dead time of the instrument is 1.3 ms, and the mixing volume is 100 $\mu$L. The reaction is followed by monitoring the absorption changes as a function of time after mixing equal volumes of the two solutions in a stopped-flow cell. Analysis of the kinetic traces was carried out with an exponential decay function using built-in software.

Radiolysis experiments were carried out using a $^{60}Co$ $\gamma$-source with a dose rate of 60 Gy/min (1 Gy = 1 J $kg^{-1}$). $^{\bullet}OH$ radicals were generated by the radiolysis of $N_2O$ saturated aqueous solutions, where radiolysis of water produces primary radicals, $H^{\bullet}$, $^{\bullet}OH$, and $e^-_{aq}$, and in the presence of $N_2O$, $e^-_{aq}$ is quantitatively converted in to hydroxyl radicals ($N_2O + e^-_{aq} \rightarrow N_2 + {}^{\bullet}OH + OH^-$).[21,22]

Kinetics of singlet oxygen reactions with selenourea was studied using transient luminescence spectrometer (TL900) from Edinburgh Instruments, U.K. Singlet oxygen was generated by photoexcitation (532 nm) of 120 $\mu$M hematoporphyrin solutions ($OD_{532} = 0.43$) in acetonitrile.[23] After laser excitation, the decay profile of singlet oxygen emission was monitored at 1270 nm with the help of liquid nitrogen cooled germanium detector. Change in the lifetime of singlet oxygen was monitored in the presence of 0.1−0.4 mM selenourea to determine the singlet oxygen-quenching rate constant. Enough care was taken to see that all the solutions contained the same amount of hematoporphyrin. For determination of the size of the selenium particles prepared by singlet oxygen reaction, the solutions of hematoporphyrin and selenourea were prepared in 10 mM SDS in water and the samples were subjected to photolysis with 532 nm light.

To prepare nanoselenium free from the reactants, the BSA and SDS stabilized selenium particles prepared by the reaction of selenourea (concentration in millimolar range) with excess $H_2O_2$ in the presence of stabilizer were subjected to extensive dialysis using dialysis membrane for at least 48 h in aqueous medium, by changing the medium after every 4 h. The concentration of nanoselenium in the dialyzed samples was estimated according to the reported procedure.[24,25] Briefly, the samples were digested with aquaregia and evaporated to dryness. Excess nitrate in the sample was decomposed by perchloric acid, and selenium was estimated using 2,3-diaminonaphthalene by fluorescence method.[24,25]

DLS measurements were carried out on a Malvern 4800 Autosizer employing 7132 digital correlator. The light source is an Ar-ion laser operated at 514.5 nm with a maximum output power of 2 W. Measurements were made at 90° scattering angle and at variable laser power depending on the scattering intensity. Typically, 250−500 mW laser power is used. The intensity correlation function of scattered light is analyzed by the method of cumulants using the mean and variance of the distribution as the fitted parameter.[26] The cumulant method expands the correlation function in terms of the moments of the distribution. The first two moments give the mean and variance of the distribution, respectively. Inverse Laplace transformation of the data was also performed using the CONTIN algorithm to obtain the nature of polydispersity in distribution.[27,28] The diffusion coefficients ($D$) of the scatterers are related to the relaxation time ($T$) of the correlation function by the relation $1/T = 2Dq^2$, where $q$ is the magnitude of the scattering vector. The hydrodynamic diameters of the particles are calculated from the $D$ values using Stokes−Einstein equation. For monomodal distribution, the average diameter obtained from cumulant results are used to represent the mean of the distribution, while for multimodal distribution the CONTIN results are preferred.

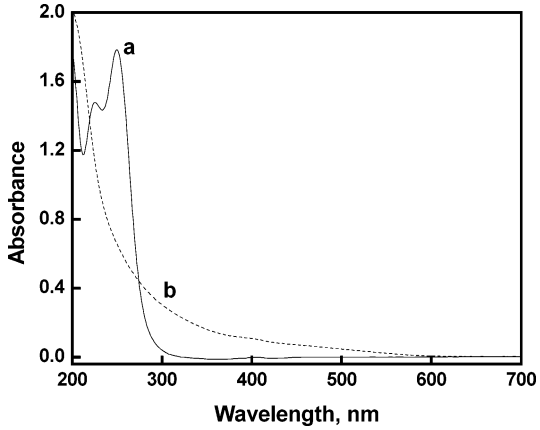


**Figure 1.** Absorption spectra of (a) 200 $\mu$M selenourea and (b) Se nanoparticle formed by mixing 200 $\mu$M selenourea with 20 mM $H_2O_2$ and stabilized by 10 mM SDS.

## Results and Discussion

**Reactions of Selenourea with $H_2O_2$, Peroxynitrite, and Singlet Oxygen.** Initially, absorption spectral changes were monitored to follow the formation of nanoselenium. Change in the absorption spectra of 200 $\mu$M selenourea in the presence of 10 $\mu$M SDS after mixing with $H_2O_2$ at pH 7 is shown in Figure 1a,b. It can be seen that selenourea is completely consumed in the presence of $H_2O_2$, with development of new absorption extending up to 500 nm due to the formation of selenium particles. Similar absorption spectral changes were observed with other oxidants also (results not shown). The rate constants for these reactions were determined by stopped-flow spectrometer by following the time-dependent changes in the absorbance at 250 nm due to selenourea over a time period of a few hundred seconds after mixing selenourea with hydrogen peroxide. The absorption−time plot shows a fast and slow component (figure not shown), and the fast component could be fitted to an exponential function and the observed rate constant ($k_{obs}$) was found to depend on the concentration of both selenourea and $H_2O_2$. Under pseudo-first-order conditions variation in $k_{obs}$ can be followed as a function of either selenourea or $H_2O_2$ concentration. Figure 2a gives the linear dependency of $k_{obs}$ as a function of $H_2O_2$ concentration, at a fixed concentration of selenourea (100 $\mu$M), from which the rate constant for the reaction of selenourea with hydrogen peroxide was determined to be $(2.3 \pm 0.1) \times 10^{-2}$ $M^{-1}$ $s^{-1}$. The slow component did not show any observable dependency on the reactants. Similarly

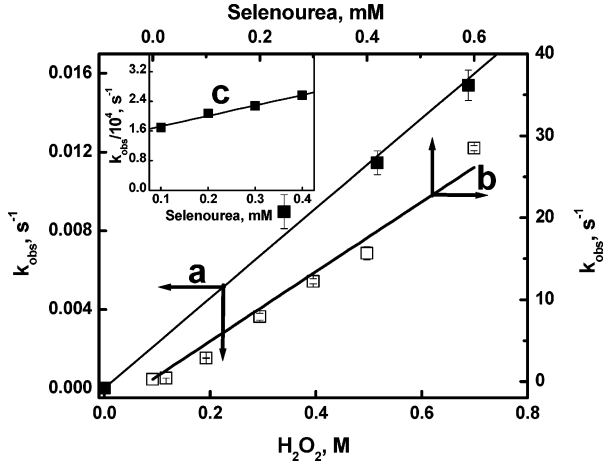


**Figure 2.** Linear plots showing the variation of observed first-order rate constant as a function of (a) $H_2O_2$ concentration on mixing 100 $\mu$M selenourea with different concentrations of $H_2O_2$, (b) selenourea concentration on mixing different concentrations of selenourea with 400 $\mu$M peroxynitrite, and (c) selenourea concentration on reaction with singlet oxygen.

the reaction of selenourea with peroxynitrite was followed using stopped-flow spectrometer by following the decay of peroxynitrite at 302 nm in the presence and absence of selenourea. The $k_{obs}$ thus obtained was plotted against the concentration of selenourea to obtain a linear plot (Figure 2b), and from the slope the rate constant was estimated to be $(4.3 \pm 0.2) \times 10^4$ $M^{-1}$ $s^{-1}$.

Similarly the rate constant for the reaction of singlet oxygen with selenourea was determined by following the change in the decay of singlet oxygen emission at 1270 nm in the absence and in the presence of selenourea. The $k_{obs}$ was plotted as a function of selenourea concentration (Figure 2c), to obtain a linear plot and from the slope the bimolecular rate constant was estimated to be $(1.9 \pm 0.4) \times 10^8$ $M^{-1}$ $s^{-1}$. Because selenourea is soluble in water, addition of SDS or BSA did not affect the above rate constants significantly within the range of concentrations employed in our studies. In the control experiments no reaction was observed between BSA or SDS with selenourea.

**Formation of Elemental Selenium on Oxidation of Selenourea.** In all the experiments discussed above, elemental red selenium was formed as one of the products. Treatment of selenourea solutions with any of the above oxidants turned the solutions into pink, which during the course of time changed to intense red and finally to a gray precipitate. Although formation of elemental selenium was observed under both aerated and nitrogen saturated conditions, the yield was more under aerated conditions. Since elemental selenium of nanometer size is known to be more biologically active than other selenium compounds,[10−13] attempts have been made to stabilize the selenium nanoparticles and study their redox reactions.

The possible mechanistic processes leading to the formation of selenium on oxidation of selenourea by the above oxidants is presented in Scheme 1. The scheme is based on the mechanism suggested for formation of elemental sulfur from thiourea.[29]

The initially formed pink-colored transparent solutions could be stabilized for days with the addition of proteins such as BSA or surfactants such as SDS, as these solutions are known to stabilize selenium particles by forming either protein conjugates or by the adsorption of surfactants on particle surface.[10,30] In the case of $^{\bullet}$OH radical ($\gamma$-radiation) induced oxidations, no stabilizer could be added, as the stabilizers themselves are good $^{\bullet}$OH radical scavengers. Therefore stabilizers could be added only after the irradiation is stopped. Thus irradiated aqueous selenourea solutions were treated with both BSA and SDS immediately (in less than 5 min), and these samples could be stabilized for several days without any appreciable change in size. For the reactions of other oxidants, samples of selenourea pretreated with either BSA or SDS were subjected for reaction with oxidants such as $H_2O_2$, peroxynitrite, and singlet oxygen. No significant change in the reactivity was observed with the addition of these stabilizers.

**Characterization of the Size of Elemental Selenium.** Random Brownian motion of the colloidal Se particles leads to fluctuations in the intensity of light scattered by the colloidal solution. The time scale of these fluctuations is a measure of the hydrodynamic size of the particles. Quantitative estimate

**SCHEME 1: Possible Mechanism for the Formation of Elemental Selenium by the Reaction of Various Oxidants with Selenourea**

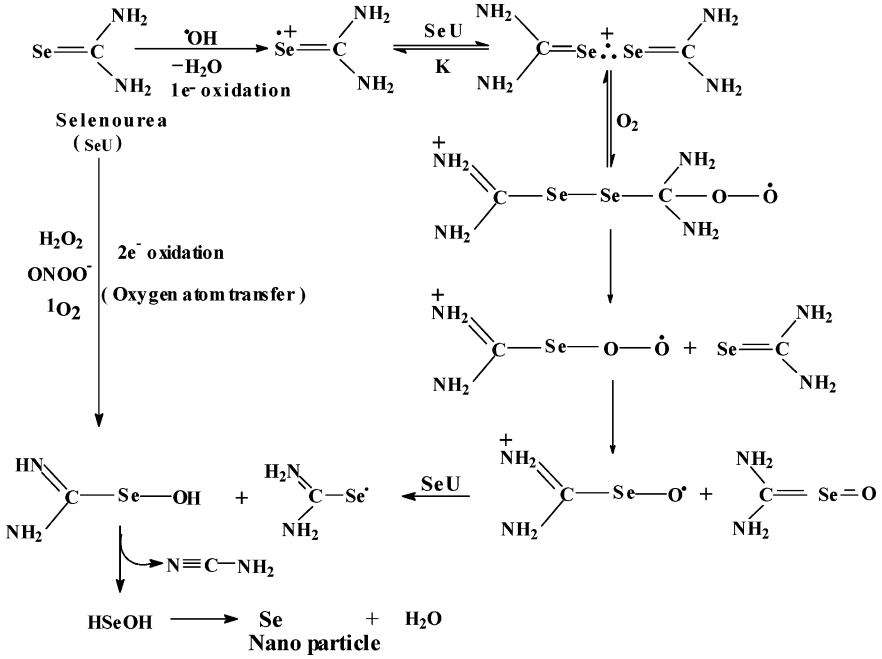

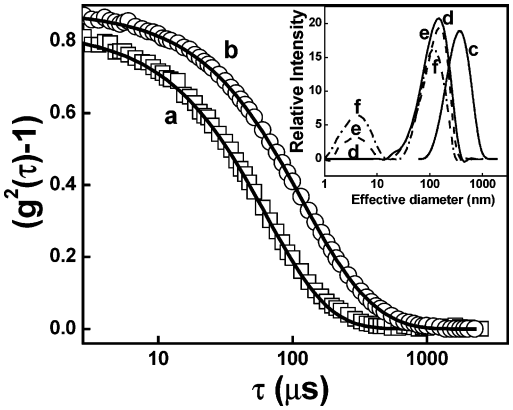


**Figure 3.** Variation of normalized intensity correlation function ($g^2(\tau) - 1$) with time for Se nanoparticles prepared by •OH radical reaction with different concentrations of selenourea (a, 50 $\mu$M; b, 200 $\mu$M) (•OH radicals produced by $\gamma$-irradiation). The solid lines are fitted to the data by the method of cumulants. The inset shows the size distribution of Se nanoparticles prepared by oxidation of 25 $\mu$M selenourea with 1.4 mM $H_2O_2$ at different concentrations of BSA (c, 0 $\mu$M; d, 10 $\mu$M; e, 100 $\mu$M; f, 200 $\mu$M).

of the time scale of fluctuations in intensity can be obtained from the autocorrelation of the scattered intensity [$g^2(\tau)$] from the solution. Hydroxyl radical reaction of aqueous selenourea in the presence of oxygen produced Se nanoparticles that are stabilized by the addition of SDS. Parts a and b of Figure 3 show representative plots of the normalized intensity correlation function ($g^2(\tau) - 1$) at 50 and 200 $\mu$M selenourea, respectively. The shift of the correlation function to higher times with an increase in selenourea concentration is an indication of the increase in the relaxation time, which in turn reflects the increase in the average size of Se nanoparticles. For narrow polydispersity, the correlation function can be expressed using the method of cumulants.

The solid lines in Figure 3a,b show the fit to the measured data using cumulants, and the corresponding average hydrodynamic diameter increased with selenourea concentration, from 37 nm at 50 $\mu$M selenourea to a value of 52 nm at 200 $\mu$M selenourea. The size distribution is monomodal in nature with relatively small polydispersity (polydispersity index (PI) < 0.1, PI = variance/(mean)$^2$). In the absence of any stabilizer the average size and the polydispersity of the particles are much higher (55−71 nm and PI = 0.15). The size distribution is practically unaffected with changes in absorbed dose of 65−325 Gy or hydroxyl radical concentrations.

Detailed studies on the characterization of Se nanoparticles prepared using $H_2O_2$ as the oxidant in the presence of SDS or BSA as the stabilizer have been made. In the absence of any stabilizer, $H_2O_2$ produced highly polydisperse and larger particles of Se with average size of ∼325 nm (Figure 3c), while the presence of stabilizers such as SDS or BSA decreased the particle size to ∼100 nm. The size distribution depends very much on the concentration of oxidant and stabilizers. When SDS is used as the stabilizer, a nonlinear variation of particle diameter is observed as a function of SDS concentration. For 25 $\mu$M selenourea and 1.4 mM $H_2O_2$, a unimodal distribution of sizes with a large polydispersity (PI = 0.4) is observed as SDS concentration is varied from 3 to 9 mM. The average diameter increased from 110 to 170 nm as SDS concentration approached 6 mM and then further decreased to 90 nm at SDS concentration of 9 mM. In the presence of BSA, the size distribution is bimodal in nature with a major peak centered at around 100 nm and a minor distribution at around 10 nm. Parts a−f of Figure 3 show the size distribution in the absence and in the presence of 10, 100, and 200 $\mu$M BSA, respectively. The intensity of the minor peak increased with an increase in $H_2O_2$ or BSA concentrations, while the peak positions remained approximately the same, indicating no significant change in the average size with BSA.

Peroxynitrite reactions with selenourea also produced selenium particles, but the particles were found to be much more polydisperse. Solutions containing a peroxynitrite concentration of 1.1 mM, 10 mM SDS, and 25 $\mu$M selenourea produced large polydisperse (PI = 0.37) population of Se nanoparticles. The results indicate that a lower concentration of selenourea (<100 $\mu$M) or peroxynitrite (0.5−3 mM) is favorable for the formation of small Se particles (size 66−90 nm). Similarly, singlet oxygen reactions with selenourea produced Se particles ranging in size from 20 to 170 nm in the presence of SDS, the size varied with the initial singlet oxygen yield, and the particles are highly polydisperse (Table 1).

The above result suggests that the size of selenium particles depends mainly on the concentration of selenourea and oxidant. Also, the presence of stabilizer such as SDS or BSA helps in preventing the particles undergoing flocculation. Parts a−c of Figure 4 summarize the variation in average size of particles with a change in concentration of $H_2O_2$, BSA, and selenourea, respectively. Of all the reactions, hydroxyl radical reaction produced the smallest particles of selenium (∼37 nm), while fairly high concentration (>10 mM) of $H_2O_2$ was required to generate small size selenium particles (∼37 nm). An attempt has also been made to correlate the rate constant for the reaction of selenourea with the oxidant and the size of the selenium particle. The results listed in Table 1 suggest that oxidants with high rate constant produce smaller particles with low polydispersity. However this alone does not explain the size variation, probably other factors such as reactivity, which is a product of rate constant and concentrations of the reactants and mode of initial electron transfer may also play an important role in determining the size and polydispersity of the particles. It is known that hydroxyl radicals react by electron transfer with selenourea;[17] however the mechanism of reaction of other oxidants is not known. $H_2O_2$ is a mild oxidant and can cause both one- and two-electron reactions,[31] while peroxynitrite is a powerful oxidant, which can cause both one- and two-electron transfer and oxygen transfer, etc.[18,32] Singlet oxygen adds to double bonds by forming hydroperoxides, which eventually lead

**TABLE 1: Reaction Rate Constants and Properties of Selenium Particles Produced by the Reaction of Selenourea with Different Oxidants**

| exp tl conditions[a] | oxidants | rate constant ($M^{-1}$ $s^{-1}$) | av size of selenium (nm) | polydispersity |
|---|---|---|---|---|
| A | hydroxyl radicals | $(9.0 \pm 0.9) \times 10^9$ | $37 \pm 1$ | 0.002 |
| B | hydrogen peroxide | $(2.3 \pm 0.1) \times 10^{-2}$ | $63 \pm 3$ | 0.19 |
| C | peroxynitrite | $(4.3 \pm 0.2) \times 10^4$ | $75 \pm 2$ | 0.371 |
| D | singlet oxygen | $(1.9 \pm 0.4) \times 10^8$ | 20−170 | 0.14−0.26 |

[a] Experimental conditions for the measurement of size and polydispersity in the above table: (A) dose = 195 Gy, [selenourea] = 50 $\mu$M, $N_2O$:$O_2$ (4:1) saturated; (B) [selenourea] = 25 $\mu$M, [BSA] = 10 $\mu$M, [$H_2O_2$] = 1.4 mM; (C) [selenourea] = 25 $\mu$M, [SDS] = 10 mM, [peroxynitrite] = 1.12 mM; (D) [selenourea] = 100 $\mu$M, [hematoporphyrin] = 120 $\mu$M, [SDS] = 10 mM.

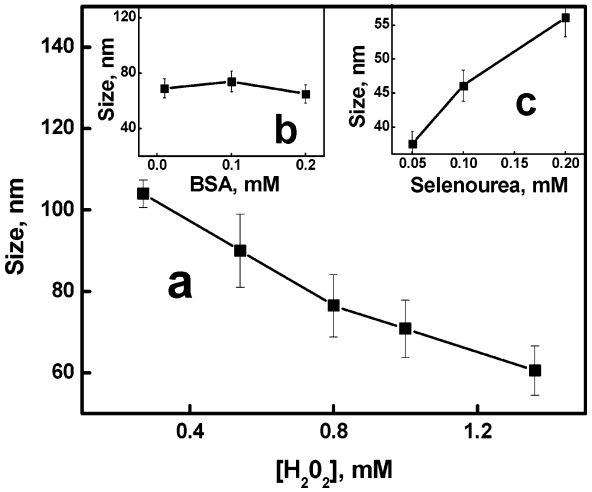


**Figure 4.** (a) Effect of $H_2O_2$ concentration on the average size of Se nanoparticle produced by the reaction of 25 $\mu$M selenourea in the presence of 10 $\mu$M BSA with 0.27−1.4 mM $H_2O_2$. (b) Effect of BSA concentration on the average size of nanoparticle formed by the reaction of 25 $\mu$M selenourea with 1.4 mM $H_2O_2$. (c) Effect of selenourea concentration on the average size of nanoparticles formed by $\gamma$-irradiation: dose, 195 Gy.

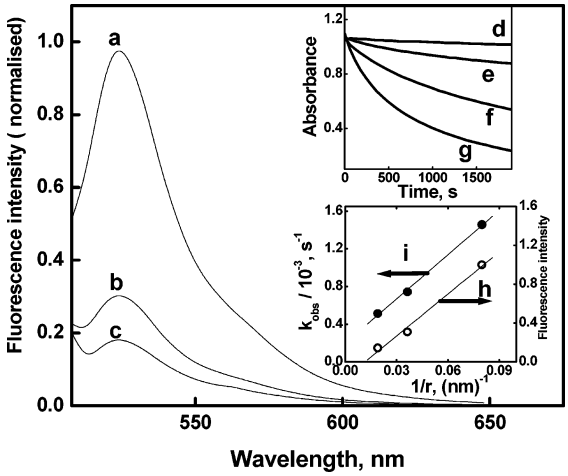


**Figure 5.** (a−c) Change in the fluorescence spectral intensity from DCF produced by the reaction of Se nanoparticles of different sizes (a, 37 nm; b, 55 nm; c, 105 nm.) with 6 $\mu$M DCFA. (Excitation wavelength = 502 nm). (d−g) Absorption−time plots showing the decay of 100 $\mu$M $ABTS^{\bullet-}$ on reaction with Se nanoparticles of varying sizes (d, control; e, 105 nm; f, 55 nm; g, 37 nm). (h and i) Variation in the normalized fluorescence intensity from DCF (○) and the observed rate constant for the decay of $ABTS^{\bullet-}$ (●) on the inverse of the radius of the nanoparticle, respectively. The inverse radius dependence suggests that the reactivity is proportional to the surface area of the nanoparticle.

to formation of free radicals.[16] Hence, it may not be possible to bring direct correlation between the size and the initial rate constant. On the basis of the present observations, it is concluded that the size of nanoselenium is mainly dictated by the amount of selenourea that actually undergoes the reaction. The more the concentration of selenourea undergoes oxidation, the larger will be the size of the particles.

**Redox Reactions of Nanoselenium.** The above solutions of nanoselenium were examined for their ability to participate in redox reactions with free radicals and molecular systems. For this, elemental selenium particles were generated by the reaction of $H_2O_2$ with selenourea. The particles produced by this reaction were kept for a few hours to allow the excess reactants to be completely consumed or decomposed (sometimes additionally by heating or dialysis), so that the initial reactants do not interfere in these studies. The concentration of the selenium was estimated as discussed in the Experimental Section. Enough care was taken to maintain the same concentration of selenium for a given set of reactions. The size of the nanoselenium was estimated by DLS measurements, and the size variation was achieved by varying the concentration of stabilizer and $H_2O_2$. Since BSA was interfering in these studies, SDS was employed as the stabilizer.

For the oxidation studies of nanoselenium, DCFA was employed. This compound is used as a marker for oxidative status in cells. It is nonfluorescent and is converted into dichlorodihydrofluorescien by slow hydrolysis, which undergoes oxidation to form a fluorescent compound DCF.[33, 34] Generally, DCFA is initially hydrolyzed by alkali to dichlorodihydrofluorescein and the hydrolyzed sample is employed for oxidation studies. But we observed that under alkaline conditions the compound undergoes autooxidation very easily, thereby producing intense fluorescence even in blank solutions and small fluorescence changes caused by the selenium particles are difficult to monitor. Therefore for these studies, nano selenium solutions (4.08 ± 0.33 $\mu$g/mL) were mixed with 6 $\mu$M DCFA solutions under neutral conditions, and after about 3 h, the solutions were excited at 502 nm and the fluorescence at 527 nm due to DCF was monitored (Figure 5a−c). Under such conditions, DCFA undergoes slow hydrolysis and the hydrolyzed sample is oxidized by nanoselenium. From Figure 5a−c, it can be seen that there is a significant increase in the fluorescence in the presence of nanoselenium, indicating that nanoselenium was able to oxidize dichlorodihydrofluorescein. Similar experiments with all the blanks such as SDS and BSA, etc., did not produce fluorescent products, confirming that this oxidizing ability arises mainly from the nanoselenium and not from the other reagents. Effect of particle size on oxidizing power of nanoselenium was also tested. For this, selenium particles of size 37−105 nm (determined by DLS) were mixed with DCFA solutions, and the results in Figure 5a−c show that the smaller the size of nanoselenium, the larger is the fluorescence intensity at a given time. This result confirms that the oxidizing power of nanoselenium depends on the size of the nanoparticle.

We also studied the reaction of nanoselenium with $ABTS^{\bullet-}$ radicals, prepared by the reported procedure.[35] It is a stable radical, dark green in color, and in the presence of compounds capable of donating electrons, it is reduced to a colorless form. Reaction with $ABTS^{\bullet-}$ radicals was monitored by following the absorbance changes at 645 nm region in the presence of nanoselenium (0.18 ± 0.05 $\mu$g/mL), as a function of time. Parts d−g of Figure 5 give time-dependent changes in the absorbance of $ABTS^{\bullet-}$ radicals in the presence of nanoselenium of varying size, and the results suggest that the decay of $ABTS^{\bullet-}$ radicals increased with decreasing particle size. This confirms that a smaller size nanoparticle is able to reduce $ABTS^{\bullet-}$ more efficiently than the larger ones. This supports the previous results by Huang et al.,[13] where it has been shown that the nanoselenium reacts with DPPH radicals and the smaller size is more reactive toward DPPH than the larger ones. In the above experiments, since the concentration of selenium is constant for a given reaction, the size dependency may either be due to a change in the number density of the particle or due to the surface area. If the number density is responsible for this, one would expect a linear variation in these above activities with $1/r^3$, and if it is due to the surface area, linearity should be observed with $1/r$, where $r$ is the radius of the particle. The above data show nearly linear variation with the inverse of particle radius (Figure

5h, and i, respectively, for DCF fluorescence and $ABTS^{\bullet-}$ decay), suggesting that the parameter correlating the redox reactivity is proportional to the total surface area of the particles. Thus, our results suggest that small-size nanoselenium has greater potential to transfer electrons to radicals and other redox systems.

## Conclusions

From the above results it can be concluded that selenourea reacts with a number of oxidants to produce elemental selenium. The selenium particles could be stabilized to nanometer size with the addition of BSA or SDS. The formation and characteristic size of the nanoselenium depends mainly on the amount of selenourea undergoing oxidation and also on the type of oxidant and the amount of stabilizer. Particles produced by the reaction of $^{\bullet}OH$ radicals generated by $\gamma$-radiation were monomodal, while those produced by the reaction of $H_2O_2$, peroxynitrite, and singlet oxygen were multimodal. These initial results suggest that small-size and less polydisperse nanoparticles are produced by more powerful oxidants. Small size is also achieved by the addition of proteins and surfactants. The stabilized selenium particles showed redox properties and participate in free radical and electron-transfer reactions. Preliminary studies indicated that such redox behavior shows size dependency, smaller size exhibiting highest activity. Under cellular systems, due to the presence of a large amount of proteins and other biomolecules, it is possible that much smaller size particles are produced under in vivo conditions. Future experiments in this direction along with theoretical calculations can exactly prove the role of size in the actual cytotoxic or cytoprotective nature of the particles.

Our preliminary studies showed that BSA-stabilized nanoselenium does not undergo further oxidation by $H_2O_2$ to selenite, as many selenium compounds are known to undergo such transformation.[31] Such reactions could prove detrimental as this can lead to production of superoxide and elevate oxidative stress by futile redox cycling. All these aspects will be addressed in the future experiments.

The present studies suggest that there is a possibility of using selenourea and its oxidation product nanoselenium in the treatment of diseases, which are linked to oxidative stress. Since selenourea has been well-tested as a radioprotector in several in vivo systems, understanding the cytotoxic or cytoprotective nature and other chemical and biochemical aspects of nanoselenium can be useful in employing selenourea and its oxidation product nanoselenium for therapeutic advantages.

**Acknowledgment.** The authors are thankful to Dr. T. Mukherjee, Head, RC & CD Division, for encouragement and support.

## References and Notes

(1) Rosenfield, I.; Beath, O. A. *Selenium: Geotoxicity, Biochemistry, Toxicity and Nutrition*; Academic Press: New York, 1964.

(2) Bock, A. In *Encyclopedia of Inorganic Chemistry*; Bruce-King, R., Ed.; Wiley: New York, 1994; Vol. 7, p 3700.

(3) Mugesh, G.; du Mont, W.; Sies, H. *Chem. Rev.* **2001**, *101*, 2125.

(4) Tapiero, H.; Townsend, D. M.; Tew, K. D. *Biomed. Pharmacother.* **2003**, *57*, 134.

(5) Badiello, R. In *The Chemistry of Organic Selenium and Tellurium Compounds*; Patai, S., Rappoport, Z., Eds.; Wiley: New York, 1986; Vol. 1, p 287.

(6) Feroci, G.; Fini, A. *J. Trace Elem. Med. Biol.* **1998**, *12*, 96.

(7) Garbisu, C.; Ishii, T.; Leighton, T.; Buchanan, B. B. *Chem. Geol.* **1996**, *132*, 199.

(8) Schlekat, C. E.; Dowdle, P. R.; Lee, B. G.; Luoma, S. N.; Oremland, R. S. *Environ. Sci. Technol.* **2000**, *34*, 4504.

(9) Sieber, F.; Daziano, J.; Gunther, W. H.; Krieg, M.; Miyagi, K.; Sampson, R. W.; Ostrowski, M. D.; Anderson, G. S.; Tsujino, I.; Bula, R. J. *Phosphorus, Sulfur Silicon Relat. Elem.* **2005**, *180*, 647.

(10) Zhang, J. S.; Gao, X. Y.; Zhang, L. D.; Bao, Y. P. *Biofactors* **2001**, *15*, 27.

(11) Zhang, J.; Wang, H.; Bao, Y.; Zhang, L. *Life Sci.* **2004**, *75*, 237.

(12) Gao, X.; Zhang, J.; Zhang, L. *Adv. Mater.* **2002**, *14*, 290.

(13) Huang, B.; Zhang, J.; Hou, J.; Chen, C. *Free. Radicals Biol. Med.* **2003**, *35*, 805.

(14) Nano Red Se (http://www. nanoport.net).

(15) Badiello, B.; Maggio, D. D.; Quintiliani, M.; and Sapora, O. *Int. J. Radiat. Biol.* **1971**, *20*, 61.

(16) Halliwell, B.; Gutteridge, J. M. C. *Free Radicals in Biology and Medicine*; Clarendon Press: Oxford, U.K., 1989.

(17) Mishra, B.; Maity, D. K.; Priyadarsini, K. I.; Mohan, H.; Mittal, J. P. *J. Phys. Chem. A* **2004**, *108*, 1552.

(18) Radi, R.; Peluffo, G.; Alvarez, M. N.; Naviliat, M.; Cayota, A. *Free Radicals Biol. Med.* **2001**, *30*, 463.

(19) Allen, A. O.; Hochanadel, C. J.; Ghormley, J. A.; Davies T. W. *J. Phys. Chem.* **1952**, *56*, 575.

(20) Pryor, W. A.; Cueto, R.; Jin, X.; Ngu-Schwemlein, M.; Squadrito, G. L.; Uppu, P. L.; Uppu, R. M. *Free Radicals Biol. Med.* **1995**, *18*, 75.

(21) Spinks, J. W.; Woods, R. J. *An Introduction to Radiation Chemistry*; Wiley: New York, 1990.

(22) Neta, P.; Huie, R. E.; Ross, A. B. *J. Phys. Chem. Ref. Data* **1988**, *17*, 1027.

(23) Keene, J. P.; Kessel, D.; Land, E. J.; Redmond, R. W.; Truscott, T. G. *Photochem. Photobiol.* **1986**, *43*, 117.

(24) Watkinson, J. H. *Anal. Chem.* **1966**, *38*, 92.

(25) Pedro, J.; Andrade, F.; Magni, D.; Tudino, M.; Bonivardi, A. *Anal. Chim. Acta* **2004**, *516*, 229.

(26) Brown, J. C.; Pusey, P. N.; Dietz, R. *J. Chem. Phys.* **1975**, *62*, 1136.

(27) Provencher, S. W. *Comput. Phys. Commun.* **1982**, *27*, 213.

(28) Provencher, S. W. *Comput. Phys. Commun.* **1982**, *27*, 229.

(29) Wang, W.; Schuchmann, M. N.; Knolle, H. P.; von Sonntag, J.; von Sonntag, C. *J. Am. Chem. Soc.* **1999**, *121*, 238.

(30) Fendler, J. H. *Membrane-Mimetic Approach to Advanced Materials*; Springer-Verlag: New York, 1994.

(31) Schumb, W. C.; Satterfield, C. N.; Wentworth, R. L. *Hydrogen Peroxide*; Reinhold: New York, 1956.

(32) Priyadarsini, K. I. *Proc. Natl. Acad. Sci. India* **2000**, *70*, 339.

(33) Glebiska, J.; Koppenol, W. H. *Free. Radicals Biol. Med.* **2003**, *35*, 676.

(34) Wrona, M.; Patel, K.; Wardman, P. *Free Radicals Biol. Med.* **2005**, *38*, 267.

(35) Erel, O. *Clin. Biolchem.* **2004**, *37*, 277.